

Diazatetraester 1*H*-Pyrazole Crowns as Fluorescent Chemosensors for AMPH, METH, MDMA (Ecstasy), and Dopamine

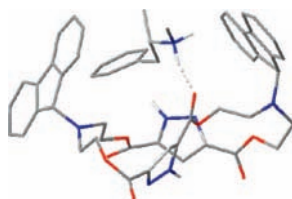
Felipe Reviriego,[†] Pilar Navarro,^{*,†} Enrique García-España,^{*,‡} M. Teresa Albelda,[‡] Juan C. Frías,[‡] Antonio Domènech,[§] María J. R. Yunta,^{||} Rubén Costa,[⊥] and Enrique Ortí[⊥]

Instituto de Química Médica, Centro de Química Orgánica Manuel Lora-Tamayo CSIC, Juan de la Cierva 3, 28006 Madrid, Spain, Instituto de Ciencia Molecular, Universidad de Valencia, Apartado de Correos 22085, 46071 Valencia, Spain, Departamento de Química Analítica, Universidad de Valencia, Dr. Moliner 50, 46100 Burjassot, (Valencia) Spain, and Departamento de Química Orgánica, Facultad de Química, Universidad Complutense de Madrid, Avda Complutense s/n 28040 Madrid, Spain

enrique.garcia-es@uv.es

Received August 5, 2008

ABSTRACT



The synthesis and steady-state fluorescence studies on the interaction with AMPH, METH, MDMA, and DA of two diazatetraester pyrazole crowns containing appended *N*-(9*H*-fluoren-9-yl) and *N*-(naphth-2-ylmethyl) functions, in a water/ethanol 70:30 mixture at physiological pH, are described.

The UN Office on Drugs and Crime recently reported that the use of (+)-amphetamine sulfate (AMPH), (+)-methamphetamine hydrochloride (METH, *ice* or *crystal*), and (±)-3,4-methylenedioxyamphetamine hydrochloride (MDMA, *ecstasy*) (Figure 1A) now exceeds that of cocaine and heroine on a global scale.¹ On the other hand, with typical patterns of abuse, the pharmacological effects of AMPH and METH, and consequently the risk associated with abuse, are different

from those of MDMA.^{2–5} Thus, deaths caused by METH intoxication have increased dramatically in the past few years due, in part, to the direct effects of intravenous METH use and/or to the secondary effects of amphetamine-induced seizures.⁶ Consequently, efficient, rapid, and simple detection methods of such drugs are of great interest.

[†] Instituto de Química Médica, Centro de Química Orgánica Manuel Lora-Tamayo CSIC.

[‡] Departamento de Química Inorgánica, Instituto de Ciencia Molecular, Universidad de Valencia.

[§] Departamento de Química Analítica, Universidad de Valencia.

^{||} Departamento de Química Orgánica, Universidad Complutense de Madrid.

[⊥] Departamento de Química Física, Instituto de Ciencia Molecular, Universidad de Valencia.

(1) http://www.unodc.org/onodc/en/global_illicit-drug_trends.html.

(2) Sulzer, D.; Sonders, M. S.; Poulsen, N. W.; Dall, A. *Prog. Neurobiol.* **2005**, *75*, 406–433.

(3) Cadet, J. L.; Krasnova, I. N.; Jayanthi, S.; Lyles, J. *Neurotox. Res.* **2007**, *11*, 183–202.

(4) McCann, U. D.; Ricaurte, G. A. *Neurosci. Biobehav. Rev.* **2004**, *27*, 821–826.

(5) (a) Kovacic, P. *Med. Hypotheses* **2005**, *65*, 90–96. (b) Chipana, C.; García-Ratés, S.; Camarasa, J.; Pubill, D.; Escubedo, E. *Neurochem. Int.* **2008**, *52*, 401–410.

(6) Cadet, J. L.; Jayanthi, S.; Deng, X. *FASEB J.* **2003**, *17*, 1776–1788, and references cited therein.

In the past decade, a wide range of efficient and selective artificial hosts for DA which afford stable complexes in organic⁷ or aqueous⁸ media have been prepared. Some of them are able to act directly as selective chemosensors or fluorescent sensors of DA.⁹ Others act as selective detectors of DA when embedded in chromatic polydiacetylene vesicles¹⁰ or when immobilized in fluorescent films.¹¹ However, the design of artificial hosts for the selective binding of amphetamines is more difficult. In this respect, several 18C6 derivatives were obtained with the aim of solving racemic mixtures.¹² Conventional methods for amphetamine detection are not based on artificial receptors. They are separation techniques some of which are based on capillary electrophoresis with laser-induced fluorescence¹³ or reversed-phase HPLC in combination with fluorescence detection.^{14,15} However, such techniques often require derivatization of the amines and expensive equipments. Recently, several strategies for optical sensing of amphetamines based either on a chromoreactant or on the analysis of charge-transfer and ion-pair complexation with some acceptors have been described.¹⁶ On the other hand, different immunosensors for amphetamine detection in blood, urine, or saliva have also been reported.¹⁷

In the search of receptors for abuse drugs, we previously reported on a series of dioxo- and diaza-substituted ester crowns, which behave as efficient hosts for AMPH and METH in DMSO solution.¹⁸ On the other hand, it was recently proven that the sodium salt of the diethyl 1*H*-pyrazole-3,5-dicarboxylate behaves as an efficient amphiphilic receptor for dopamine and amphetamines in both DMSO and aqueous solution.¹⁹ Taking into account that fluorescence detection offers a number of important advantages over other methods as high sensitivity, specificity, wide

concentration range, stability, simplicity and speed, low hazard, and low cost, we now report on two novel 1*H*-pyrazole diazatetraester crown receptors containing appended *N*-(9*H*-fluoren-9-yl) and *N*-(naphth-2-ylmethyl) fluorophoric functions (**1** and **2** in Figure 1B) that interact with AMPH, METH, MDMA, and DA and can permit their fluorescence sensing and discrimination in aqueous solution.

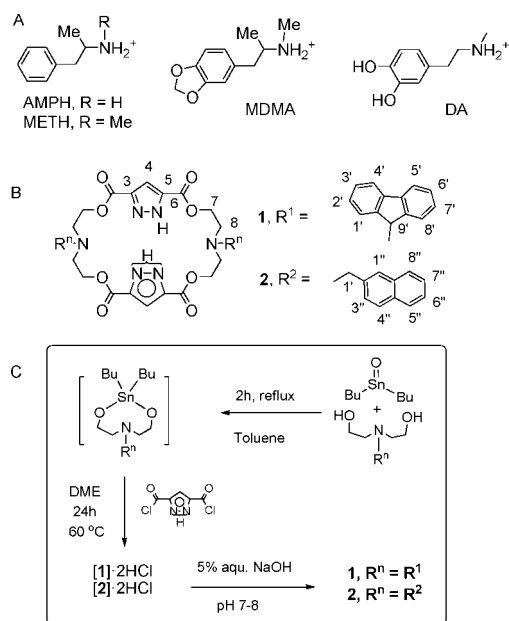


Figure 1. Compound drawings and synthetic procedure.

The synthesis of **1** and **2** was achieved as depicted in Figure 1C. The starting *N,N*-bis(2-hydroxyethyl)-9*H*-fluoren-9-ylamine and *N,N*-bis(2-hydroxyethyl)(naphth-2-ylmethyl)amine were previously prepared by reaction of 9-bromofluorene or 2-(bromomethyl)naphthalene with diethanolamine following a previously reported method.²⁰

The above aminodiols were then heated to reflux in toluene with butyltin oxide to give a mixture of stannoxanes, which were later reacted with 1*H*-pyrazole-3,5-dicarbonyl dichloride in dry dimethoxyethane at 60 °C. The corresponding reaction mixtures were then purified as indicated in the experimental part to yield compounds **1** and **2** as crystalline solids (see the Supporting Information).

Steady-state fluorometric titrations recorded in a water/ethanol 70:30 v/v mixture at variable pH ($\text{pH} = -\log [\text{H}^+]$) show different behaviors for **1** and **2**. Compound **1** displays below $\text{pH} = 6$, where both tertiary amines are protonated, an intense fluorescence due to the fluorene fragments and does not fluoresce at higher pH values. In a first approach, the quenching observed above $\text{pH} = 6$ can be attributed to a photoinduced electron transfer from the lone pair of a nonprotonated tertiary amine to the fluorophore as reported

(20) Fletcher, T. L.; Wetzel, W. H. *J. Org. Chem.* **1960**, *25*, 1348–1354.

(7) (a) Rodríguez-Franco, M. I.; San Lorenzo, P.; Martínez, A.; Navarro, P. *Tetrahedron* **1999**, *55*, 2763–2772. (b) Rübelling, D.; Schrader, T. *J. Am. Chem. Soc.* **2003**, *125*, 12086–12087.

(8) (a) Lamarque, L.; Navarro, P.; Miranda, C.; Arán, V. J.; Ochoa, C.; Escartí, F.; García-España, E.; Latorre, J.; Luis, S. V.; Miravet, J. F. *J. Am. Chem. Soc.* **2001**, *123*, 10560–10570. (b) Herm, M.; Molt, O.; Schrader, T. *Chem.—Eur. J.* **2002**, *8*, 1485–1499. (c) Escuder, B.; Rowan, A. E.; Feiters, M. C.; Nolte, R. J. M. *Tetrahedron* **2004**, *60*, 291–300.

(9) Secor, K. E.; Glass, T. E. *Org. Lett.* **2004**, *6*, 3727–3730.

(10) Kolusheva, S.; Molt, O.; Herm, M.; Schrader, T.; Jelinek, R. *J. Am. Chem. Soc.* **2005**, *127*, 10000–10001.

(11) Sindelar, V.; Cejas, M. A.; Raymo, F. M.; Chen, W.; Parker, S. E.; Kaifer, A. E. *Chem.—Eur. J.* **2005**, *11*, 7054–7059.

(12) Hyun, M. H.; Jin, J. S.; Koo, H. J.; Lee, W. *J. Chromatogr. A* **1999**, *837*, 75–82.

(13) Zhang, L.; Wang, R.; Yu, Y.; Zhang, Y. *J. Chromatogr. B* **2007**, *857*, 130–135.

(14) Tomita, M.; Nakashima, M. N.; Wada, M.; Nakashima, K. *Biomed. Chromatogr.* **2007**, *21*, 1016–1022.

(15) (a) Concheiro, M.; de Castro, A.; Quintela, O.; López-Rivadulla, M.; Cruz, A. *Forensic Sci. Int.* **2005**, *150*, 221–226. (b) Fuh, M.-R.; Lin, H.-T.; Wynn, H. T.; Lin, F.-R. *Talanta* **2002**, *58*, 1357–1363.

(16) (a) Mohr, G. J.; Wenzel, M.; Lehmann, F.; Czerney, P. *Anal. Bioanal. Chem.* **2002**, *374*, 399–402. (b) Shahdousti, P.; Aghamohammadi, M.; Alizadeh, N. *Spectrochim. Acta A* **2008**, *69*, 1195–1200.

(17) (a) Butler, D.; Pravda, M.; Guibault, G. G. *Anal. Chim. Acta* **2006**, *556*, 333–339. (b) Woodworth, A.; Saunders, A. N.; Koening, J. W.; Mayer, T. P.; Turk, J.; Dietzen, D. J. *Clin. Chem.* **2006**, *52*, 743–746. (c) Scott, S. US Patent 0224435, 2003.

(18) Reviriego, F.; Navarro, P.; Domènech, A.; García-España, E. *J. Supramol. Chem.* **2002**, *2*, 115–122.

(19) Reviriego, F.; Rodríguez-Franco, M. I.; Navarro, P.; García-España, E.; Liu-Gonzalez, E.; Verdejo, B.; Domènech, A. *J. Am. Chem. Soc.* **2006**, *128*, 16458–16459.

for related compounds.²¹ In contrast, compound **2** does not fluoresce throughout all the studied pH range (2.0–11.0). To shed some light on these different behaviors, density functional theory (DFT) calculations were performed for compounds **1** and **2** and for their monoprotonated (**1H** and **2H**) and biprotonated (**1HH** and **2HH**) species (see the Supporting Information for computational details, Figures 1S and 2S).

As illustrated in Figure 2 for compound **2**, the lowest unoccupied molecular orbital (LUMO) is located over the pyrazole moiety and one of the vicinal C=O groups both for the nonprotonated and for the protonated species. In contrast, the nature of the highest occupied molecular orbital (HOMO) changes upon protonation.

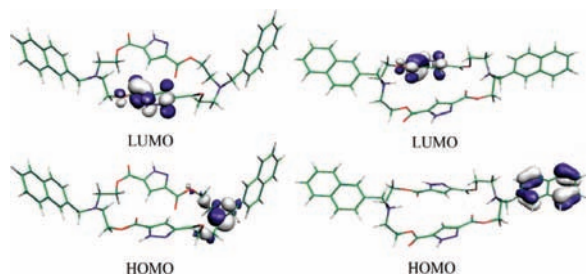


Figure 2. Electronic density contours ($0.05 e \text{ bohr}^{-3}$) calculated for the frontier molecular orbitals (HOMO and LUMO) of **2** (left) and **2HH** (right) in their singlet ground states.

The HOMO mainly involves the lone pair of the tertiary amine groups for the nonprotonated molecules and corresponds to the π HOMO of the fluorophore group in the protonated species. A similar behavior is found for compound **1**. The nature of the frontier orbitals suggests that the lowest-energy singlet excited states of **1** and **2** imply an electron transfer from the lone pair of the amine groups (nonprotonated species) or the π -orbitals of the fluorophore (protonated species) to the pyrazole groups. This photoinduced electron transfer would imply the quenching of the fluorescence over all the pH range. Time-dependent DFT (TD-DFT) calculations of the excited electronic states show that this is true for compound **2**, for which the lowest singlet excited-state always has a charge transfer (CT) nature and no fluorescence is detected. However, for compound **1**, the $\pi \rightarrow \pi^*$ excitation of the fluorene groups appears to be lower in energy than the CT states for the protonated **1HH** species formed at pH < 6 (see Table 1S in the Supporting Information). Calculations therefore predict that compound **1** should fluoresce at low pH values in agreement with experimental data.

The complexing ability of **1** and **2** toward AMPH, METH, MDMA, and DA was also examined by steady-state fluorescence measurements.

Addition of any of these drugs to receptor **1** in a 70:30 v/v water/ethanol solution at pH = 7.4 leads to an increase

of the intensity of the typical fluorene bands centered at 377, 396, and 416 nm without producing any shift in their wavelength (Figure 3). It is interesting to remark that a nonstructured red-shift band attributable to the formation of an intramolecular excimer appears around 450 nm.

Analysis of the fluorescence data for the different **1**/drug systems studied with the computer program HYPERQUAD²² allows for establishing the formation of adducts of 1:1 stoichiometry and deriving the binding constants which are presented in Table 1. Considering the large water content of the solvent used, it can be concluded that the values obtained for the binding constants are very high. It is also interesting to remark that the binding constants for the four systems are close between them; the selectivity expressed as the quotient of the binding constants at pH = 7.4, shows modest values of just around 3-fold [$K_a(\text{DA})/K_a(\text{AMPH}) = 2.5$; $K_a(\text{DA})/K_a(\text{METH}) = 3.1$; $K_a(\text{DA})/K_a(\text{MDMA}) = 2.8$]. However, the observed small differences suggest an interaction between the ammonium group of the studied amines and the ligand, since the primary ones lead to more stable complexes than the secondary ones of similar structure.

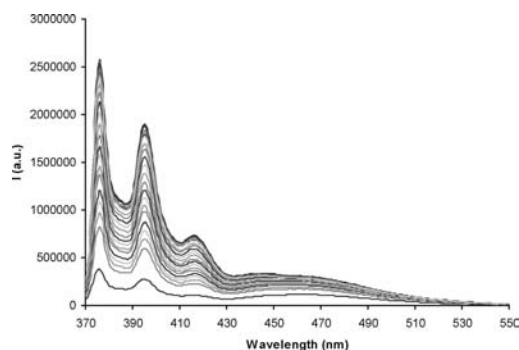


Figure 3. Variation in the emission spectra of **1** upon successive additions of METH variations: [**1**] = 10 μM , [METH] = 1–100 μM , $\lambda_{\text{exc}} = 342 \text{ nm}$.

In the case of **2**, while addition of either (+)-AMPH or (+)-METH produces neither increases nor shifts in the emission of the naphthalene fluorophore, addition of (\pm)-MDMDA or DA leads to a significant increase in fluorescence.

However, in the system **2**-(\pm)-MDMA excitation at 300 nm leads also to the excitation of the 1,3-benzodioxole moiety of MDMA. Therefore, the emissive character of MDMA was taken into consideration in the fitting of this system. Although not so overlapped, some emission of DA is achieved by excitation at this wavelength and this was also considered. The calculated constants are shown in Table 1B. In this case, the presence of hydroxy or methylenedioxy substituents affect significantly the values of the stability constants (see Table 1B, 2:1 substrate/receptor stoichiometry was found for the system DA/2).

Molecular modeling calculations (see the Supporting Information) provide theoretical complexation energies which

(21) Czarnik, A. W. *Fluorescent Chemosensors for Ion and Molecule Recognition*; American Chemical Society: Washington DC, 1992.

(22) Gans, P.; Sabatini, A.; Vacca, A. *Talanta* **1996**, *43*, 1739–1753.

Table 1. Experimental Binding Constants (K_a) for the interaction of **1**(A) and **2**(B) with AMPH, METH, MDMA, and DA Determined by Spectrofluorometric Titration in 70:30 H₂O/EtOH, Compared with Theoretical E_c Values

(A)		
amines	K_a	E_c (kcal/mol)
(+)-AMPH	$2.20 \times 10^5 \text{ M}^{-1}$	-12.03
(+)-METH	$1.80 \times 10^5 \text{ M}^{-1}$	-6.97
(±)-MDMA	$2.00 \times 10^5 \text{ M}^{-1}$	-9.95
DA	$5.60 \times 10^5 \text{ M}^{-1}$	-13.71
(B)		
amines	K_a	E_c (kcal/mol)
(+)-AMPH	<i>a</i>	-0.50
(+)-METH	<i>a</i>	0.66
(±)-MDMA	$1.74 \times 10^5 \text{ M}^{-1}$	-4.09
DA	$^b 3.80 \times 10^7 \text{ M}^{-2}$	-17.28

^a The change in emission was not significant. ^b This constant refers to a 2:1 substrate/receptor stoichiometry.

agree reasonably well with the experimental trend observed for the association constants (Table 1). The minimum energy conformers (Figures 4S–11S, Supporting Information) show different stabilizing hydrogen bonds, for instance, between the ammonium groups of the drugs and the O=C=O ester groups of the ligands (as in **1**–AMPH, **1**–METH, **1**–MDMA, **2**–METH, and **2**–DA), and/or between the ammonium groups of the drugs and the sp² nitrogen of the pyrazole (as in **1**–AMPH, **2**–AMPH, **2**–MDMA, and **2**–DA). Furthermore, other interactions with carbonyl groups are observed between the OH groups of the catechol moiety in **1**–DA and with the oxygens of the methylenedioxy group in **1**–MDMA.

It is interesting to point out that despite the relatively poor thermodynamic selectivity found in the case of **1** (vide supra), the changes in the fluorescence emission observed for the different **1**/drug systems are really significant. The Stern–Volmer plots for the four drug/**1** systems studied show different responses (Figure 4).

METH yields the largest variations in fluorescence for a given amount of added drug followed by AMPH, MDMA, and DA. Interestingly enough, this behavior, which is presented in the inset of Figure 4 as the percentage of response variation for the addition of an equimolar amount of drug, does not follow the thermodynamic sequence. While METH produces over a 350% increase in the response, DA, which is the drug with the highest constant (Table 1), yields below a 100% increase in intensity at this pH.

This lack of parallelism between the changes in fluorescence and binding strength have been already observed in a number of different systems²³ and it is usually related with

(23) Clares, M. P.; Lodeiro, C.; Fernandez, D.; Parola, A. J.; Pina, F.; García-España, E.; Soriano, C.; Tejero, R. *Chem. Commun.* **2006**, 3824–3826.

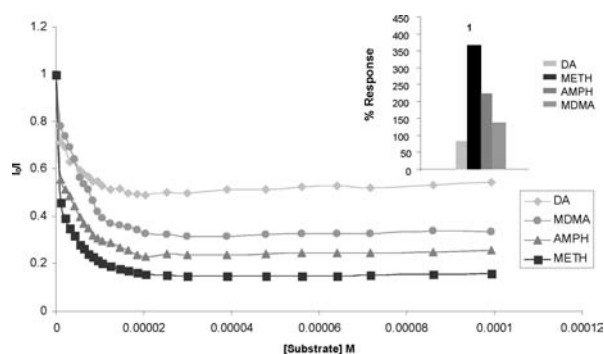


Figure 4. I_0/I vs substrate concentration plots obtained for compound **1**. The inset represents the response in percentage for the addition of an equimolar amount of AMPH, METH, MDMA, and DA to receptor **1**.

the relative disposition of key groups of receptor and substrate in the formed adduct.

Taking into account the sensitivity of the equipment and a plot of the fluorescence intensity variation with respect to the concentration of the substrate (Figure 3S), the detection limit values DA 67.0 ppb, METH, 1.3 ppb, AMPH 7.4 ppb, and MDMA 8.0 ppb can be calculated.

Receptor **2** would completely discriminate MDMA over AMPH and METH (Figure 3S). However, the analysis of the naphthalene emission is hampered by the overlapping of the MDMA and DA emissions.

Although the mechanism by which the fluorescence is restored in the presence of the drugs is still under study, preliminary studies suggest that interactions between the ammonium groups of the receptors and the imine nitrogen and the C=O groups of the esters should be a key factor in this respect.^{24,25} Further studies are currently being carried out in order to unravel the mechanisms by which these very promising molecules operate.

Acknowledgment. This work was supported by the Spanish Ministry of Science and Innovation (CTQ2006-15672-CO5-01, CTQ2006-15672-CO5-05, CTQ2006-14987-CO2-O2, CSD2007-000101) and the Generalitat Valenciana (GV/2007/141 and GVAINF 2007-051) and European FED-ER funds. J.C.F. and M.T.A. thank “Carmen y Severo Ochoa” and “Juan de la Cierva” Programmes for their respective grants.

Supporting Information Available: Experimental procedure along with full characterization for compounds **1** and **2**, Stern–Volmer plots, lifetimes, quantum yields, molecular modeling, and TD-DFT calculations. This material is available free of charge via the Internet at <http://pubs.acs.org>.

OL801732T

(24) Frahn, M. S.; Luthjens, L. H.; Warman, J. M. *Polymer* **2003**, *44*, 7933–7938.

(25) (a) Hanke, F.; Hirsch, A.; Atalick, S.; Guldi, D. *Eur. J. Org. Chem.* **2005**, 174, 1–1751. (b) Seo, Y. J.; Ryu, J. H.; Kim, B. H. *Org. Lett.* **2005**, *7*, 4931–4933.